2025 5th International Conference on High Voltage Engineering and Power Systems (ICHVEPS) | 979-8-3315-5800-0/25/$31.00 ©2025 IEEE | DOI: 10.1109/ICHVEPS66913.2025.11351260

Modelling and Evaluation of Electrical Power in Mass Rapid Transit (MRT) Systems using Field Oriented Control (FOC)

1st Antonius Doddy Tyas Prasetyo
Electrical Engineering, Faculty of Engineering
Christian University of Indonesia (UKI)
East Jakarta, Indonesia
antonius.prasetyo@uki.ac.id

2nd Tahan Lumban Tobing
Master's Program in Electrical Engineering
Christian University of Indonesia (UKI)
East Jakarta, Indonesia
tahan.tobing@uki.ac.id

3rd Dery Elfando
Electrical Engineering, Faculty of Engineering
Christian University of Indonesia (UKI)
East Jakarta, Indonesia
dery.elfando@uki.ac.id

4th Eva Magdalena Silalahi
Electrical Engineering, Faculty of Engineering
Christian University of Indonesia (UKI)
East Jakarta, Indonesia
eva.silalahi@uki.ac.id

***Abstract*—A key component of MRT operation as a contemporary urban transportation system is the dependability and efficiency of the electric power system. The traction system, particularly the three-phase induction motor that powers the train's primary propulsion, places the largest and most dynamic strain on this system. The control mechanism used has a significant impact on the performance of this motor. Therefore, this study's goal is to thoroughly investigate the use of inverter technology using a vector control (VC) approach, also known as field-oriented control (FOC), and assess how it affects important parameters in the MRT's power system. Using extensive mathematical modeling and dynamic simulations based on MATLAB / Simulink software, the methodology of this study takes a quantitative approach. A three-phase induction motor acting as the load, a field-oriented control (FOC), a pulse width modulation (PWM) inverter, and the power supply make up the model. The simulation aims to simulate the actual operating conditions of the train. According to simulation results, the system uses about equal amounts of active power (P) and reactive power (Q), 217.8 kW and 217.6 kVAR, respectively. A lagged power factor of 0.707 is obtained from these figures. For large-scale power systems, this figure is still within an acceptable operating range, although it shows a considerable reactive power consumption. The outstanding quality of the present is one of the most important conclusions of the study. A remarkably low current Total Harmonic Distortion (THDi) value of 0.288% was found through harmonic analysis. The international standard IEEE 519 2014 recommends a maximum threshold of 5%, which is much lower. The use of a vector-controlled inverter in the MRT train drive system has demonstrated that it can precisely regulate motor torque and speed while preserving high power quality. By preventing harmful harmonic distortion from being introduced into the MRT grid by the traction system, the low THDi improves the overall stability, effectiveness, and dependability of the system.**

***Keywords*—Field-oriented control (FOC), inverter, MRT power system, induction motor, power quality**

I. Introduction

In an attempt to increase operational dependability and energy efficiency, the MRT electrical system has emerged as a major area of study. Numerous in-depth improvements and research into energy consumption optimization, power quality management, and the dependability of the MRT electrical infrastructure have become necessary due to the growing passenger traffic and the need for sustainable mobility.

System-level efficiency has been studied extensively in the past. Examples include integrating Energy Storage Systems (ESS) to stabilize voltage and lower peak loads [1] [2] and optimizing train timetables to maximize regenerative braking energy exchange [3] [4]. In addition, power quality analysis—including harmonics and voltage drops—has emerged as a crucial area of attention for preserving system dependability [5] [6]. A three-phase induction motor is at the center of this traction system, and the control strategy employed directly affects both the drive efficiency and the power profile that is taken from the grid. Research has indicated the importance of determining the optimal operating point of the traction motor in terms of efficiency [7].

However, most research focuses on macro-level techniques (schedules and ESS). There is a gap in the body of research that fully models and simulates FOC-based drive systems to evaluate their power performance, and further research is required to fully link the use of contemporary motor control approaches, such as FOC or Vector Control, to their quantitative effects on power quality measures in the context of dynamic MRT train loads.

Thus, the main goal of this study is to evaluate the performance of a three-phase induction motor drive system in an MRT application utilizing the FOC approach. This study

focuses on the quantitative assessment of the power factor, reactive power, active power consumption, and the associated total harmonic distortion of current (THDi). One of the limitations of the study is that it only used MATLAB/Simulink simulations to analyze motor parameters and train loads, using data from the study [8]. Regenerative braking and interactions with other train units were not examined.

This study is expected to improve the knowledge of the power characteristics of contemporary driving systems and how they affect the overall power quality of the MRT electrical system. The following order will be used to describe this paper: suggested technique, findings and discussion, and conclusion.

II. Suggested Approach

A. Equation for Mechanical Power of a Train

The equation for the mechanical power of the train, as derived from [8]

$$P = \frac{1000}{3600} \cdot \frac{F_t\, v}{\eta} \tag{1}$$

where:
F_t = total tensile force
v = train speed
eta = motor efficiency
F_t consists of gradient, wind resistance, track curve, and train acceleration. The discussion related to equation (1) can be reviewed again in [8].

B. Field Oriented Control / Vector Control Method

High dynamic responsiveness is achieved through the use of vector control or field-oriented control. The equation can be represented as follows using an induction motor or machine's fundamental equivalent circuit:

$$\overline{V}_s = R_s\, \overline{I}_s + j\omega_e L_{ls}\, \overline{I}_s + \overline{E}_m \tag{2}$$

If $\overline{E}_m$ is taken as a reference, then

$$\overline{I}_s = I_r - jI_m \tag{3}$$

where

$$I_r = \frac{E_m}{R_r}\, s \tag{4}$$

and

$$I_m = \frac{E_m}{\omega_e L_m} \tag{5}$$

The induced emf voltage can be expressed as

$$E_m = \lambda\, \omega_e \tag{6}$$

λ denotes the rated linkage flux. Substituting equation (6) into equations (4) and (5) results in the following equation:

$$I_r = \frac{\lambda}{R_r}\, s\, \omega_e \tag{7}$$

and

$$I_m = \frac{\lambda}{L_m} \tag{8}$$

The torque of the engine is provided by

$$T_d = \frac{3pI_r^2}{\omega_s} \cdot \frac{R_r'}{s} = \frac{3pI_r^2 R_r'}{\omega_{\text{slip}}} \Rightarrow T_d = 3p\lambda I_r \tag{9}$$

The stator current is as follows

$$\overline{I}_s = I_r - jI_m = I_q - jI_d \tag{10}$$

1) Speed Loop: Electromagnetic torque generated by the motor in the speed loop, or the rotational force, causes the motor to rotate, expressed as:

$$T_d = 3p\lambda^{\text{rms}} I_r^{\text{rms}} = \tfrac{3}{2} pL_m I_d I_q \tag{11}$$

where:
p = the number of pole pairs in the motor, which determines its rotational speed
Lm = mutual inductance between the stator and rotor
Given that p, Lm, and Id are stable quantities for motor (assuming constant flux), they can be combined into a single constant, K_T, which represents the motor torque constant, as shown in equation (14).

$$K_T = \tfrac{3}{2}\, pL_m I_d \tag{12}$$

The two formulas ((11) and (12)) are essential for the precise torque control of an induction motor through FOC.

2) Loop Current (Id, Iq): There are two parts to the stator current:

- The direct current component, $I_d = I_m$, indicates the flux-producing current component that causes the core's magnetization.
- $I_q = I_r$ denotes the torque-producing current component.

An induction motor or machine (IM) can attain the same dynamic performance by managing two stator current components individually. For precise current reference tracking and to minimize current and torque ripple, this current loop must be properly tuned.

FOC control is naturally expected to reduce "unused" real power by managing Id, which in turn minimizes reactive power (optimizes power factor).

C. Simulation Circuit Block Diagram

The simulation circuit in Figure 1 illustrates the integration of each component and is a simplified version of the simulation circuit in MATLAB Simulink. The receiving substation (RSS) provides a traction substation, which supports the overhead contact system (OCS), which provides v_dc. In the 'FOC+PWM+Inverter' block diagram, v_dc represents the inverter's input/output voltage. '3 Phase Induction Motor' block uses the block diagram output to determine the stator current (Is_abc) and motor speed (v_m). The Id and Iq components are determined by converting the stator current.

The motor's actual speed relative to the speed reference (using data from [8], but assuming that the distance interval from 0 to 8km elevates/ascent).

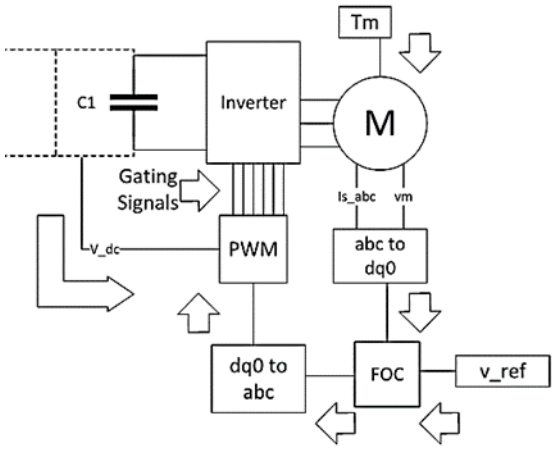

Fig. 1. Simulation circuit's block diagram

III. Outcome and Discussion

A. Elevation Profile of the MRT Line

Track elevation versus distance is plotted in Figure 2, where gradient (G) is represented as a percentage (%), station locations are represented by red dot symbols, and turning points are represented by x symbols. While the profile from 8km to the end (16km) is based on data from [8], the profile from 0km to 8km is constructed using a linear ascent.

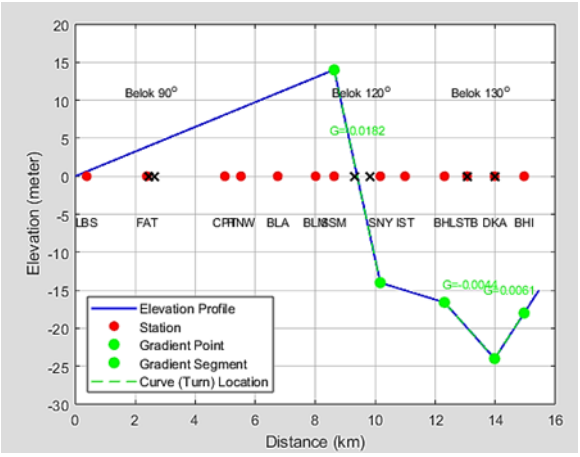

Fig. 2. MRT line profile (elevation (m) as a function of distance (km))

B. Profile of DC Voltage

A graph of the DC bus voltage (V) vs distance (km) is displayed in Figure 3. Throughout the simulation, the nominal system voltage of 1500 Vdc was consistently maintained within the specified tolerance range, which extends from the lower limit of 1000 Vdc to the upper limit of 1800 Vdc.

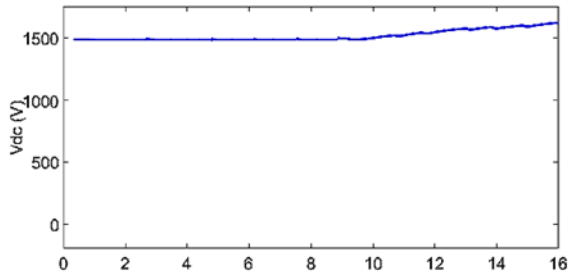

Fig. 3. Voltage profile (Vdc) as a function of distance (km)

C. Speed of the Motor / Rotor

Figure 4 illustrates the acceleration graph, depicting the speed of the motor/rotor (blue line) compared to its reference (red line). Depending on the situation, the reference may be either forward or backward. The MRT system encounters regenerative braking as it gets closer to the destination station at intervals of 8 to 16 km, as shown by the MRT track profile (Figure 2). The MRT track profile graph in Figure 3 also has an impact on the DC voltage, confirming that regenerative braking does take place during these intervals.

A cycle of acceleration and deceleration may be indicated by this recurrent speed reduction behavior, depending on the expected operating profile (e.g., MRT track profile in Figure 2). The quick deceleration phase (sharp decreases in the blue and red lines) in this case may be an indication of regenerative braking as the MRT train approaches a station or decelerates to a stop. This is consistent with the effect on DC voltage (Figure 3) discussed earlier, which could happen during regenerative braking.

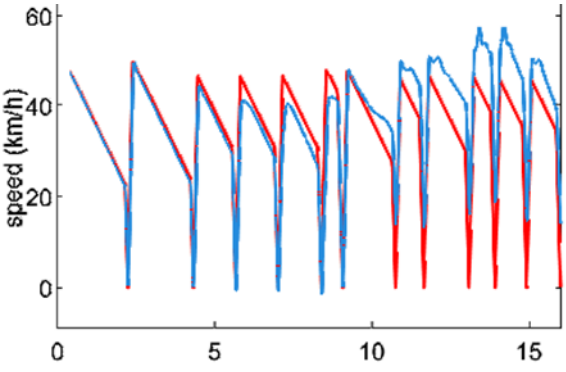

Fig. 4. Response graph for speed (km/h) as a function of distance (km)

D. Current Loop (Id, Iq)

Within the current loop, Iq regulates the torque produced by the motor, while Id regulates the magnetic flux of the motor. The graphical depiction of the control current loop is shown in figure 5 and 6, where Ki = 5800.047, lambda = 1, and Kp = 71.95 are the controller parameters used for both current loops (Id and Iq).

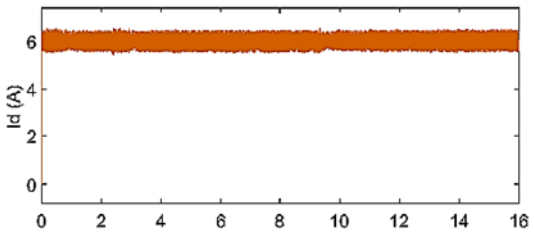

Fig. 5. Id (A) response as a function of distance (km)

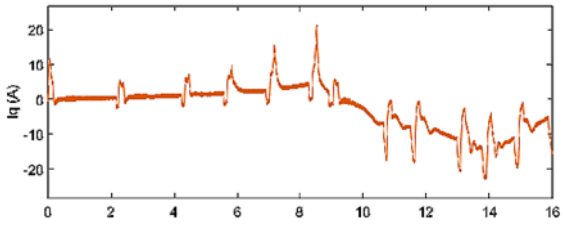

Fig. 6. Response Iq (A) as a function of distance (km)

E. Torque Electromagnetic (Te)

Figure 7 displays the motor's electromagnetic torque (Te) response as a function of distance. The rotational force delivered to the rotor is represented by this torque. Take note of the notable variations and oscillations in torque levels over time, such as times when the torque is positive (signaling forward thrust or acceleration) and times when it is negative (signaling braking or slowdown, including potential regenerative braking). Sudden torque changes will affect the motor's acceleration and could result in jerks or changes in the system's acceleration.

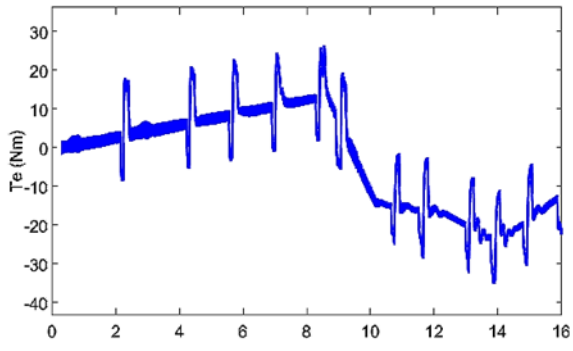

Fig. 7. Electromagnetic torque (Nm) vs distance (km)

F. Power (Reactive (Q), Active (P))

The power response observed on the 20kV bus, which comes after the 150kV bus in the MRT power distribution system, is shown in Figure 8. The system's active power (217.8kW) is displayed on the graph with the red line, while its reactive power (217.6kVAR) is displayed on the graph with the blue line. Calculations at a certain operating point show that the THDi is 0.002883, or 0.2883%, and the power factor (pf) is 0.707.

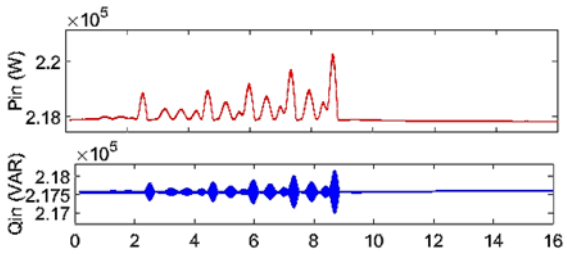

Fig. 8. 20kV bus's active power (P in kW) and reactive power (Q in kVAR) as a function of distance (in km)

IV. Conclusion

The THDi for the power quality is 0.288%. The outcome is much below the 5% termination point set by the IEEE 519-2014, indicating how effective PWM inverter technology with FOC is at reducing harmonic pollution and preserving grid stability. With 217.8 kW of active power and 217.6 kVAR of reactive power utilised, the system's power factor (PF) was 0.707. This result implies that even while a modern system's power consumption efficiency is within an acceptable operating range, it is still insufficient because a modern system should operate close to a unitary power factor. Because of the low power factor, it is quite likely that the motor is operating at full speed, which requires a considerable amount of reactive power in order to generate the magnetic flux of the motor. Consequently, although the FOC implementation effectively sustains the existing quality (low THDi), additional optimisation is necessary to enhance power factor and power efficiency.

References

[1] J. Chen, Y. Zhao, M. Wang, K. Wang, Y. Huang, and Z. Xu, "Power Sharing and Storage-Based Regenerative Braking Energy Utilization for Sectioning Post in Electrified Railways," *IEEE Trans. Transp. Electrific.*, vol. 10, no. 2, pp. 2677–2688, Jun. 2024, doi: 10.1109/TTE.2023.3295089.

[2] B. Zhang *et al.*, "Impact of On-Board Hybrid Energy Storage Devices on Energy-Saving Operation for Electric Trains in DC Railway Systems," *Batteries*, vol. 8, no. 10, art. 167, Oct. 2022, doi: 10.3390/batteries8100167.

[3] C. Wu, S. Lu, F. Xue, L. Jiang, M. Chen, and J. Yang, "A Two-Step Method for Energy-Efficient Train Operation, Timetabling, and Onboard Energy Storage Device Management," *IEEE Trans. Transp. Electrific.*, vol. 7, no. 3, pp. 1822–1833, Sep. 2021, doi: 10.1109/TTE.2021.3059111.

[4] D. Sadiq, "Review of Energy Storage Systems in Regenerative Braking Energy Recovery in DC Electrified Urban Railway Systems: Converter Topologies, Control Methods & Future Prospects," TechRxiv preprint, Sep. 2021, doi: 10.36227/techrxiv.16699942.v1.

[5] J. L. Afonso *et al.*, "A Review on Power Electronics Technologies for Power Quality Improvement," *Energies*, vol. 14, no. 24, art. 8585, Dec. 2021, doi: 10.3390/en14248585.

[6] R. S. Salles and S. K. Rönnberg, "Review of Waveform Distortion Interactions Assessment in Railway Power Systems," *Energies*, vol. 16, no. 14, art. 5411, Jul. 2023, doi: 10.3390/en16145411.

[7] C. Fu, P. Sun, J. Zhang, K. Yan, Q. Wang, and X. Feng, "An energy-efficient train control approach with dynamic efficiency of the traction system," *IET Intell. Transp. Syst.*, vol. 17, no. 6, pp. 1182–1199, Jun. 2023, doi: 10.1049/itr2.12351.

[8] T. L. Tobing *et al.*, "Multi-Objective Optimization to find the Location and Power Capacity of DC Traction Substations to supply the MRT System with Multi Train," *Int. J. Electr. Eng. Inform.*, vol. 15, no. 3, pp. 483–494, Sep. 2023, doi: 10.15676/ijeei.2023.15.3.8.